Brazilian Journal of Physics (2022) 52: 19
https://doi.org/10.1007/s13538-021-01025-z

STATISTICAL

Strong Dynamical Trappings Originating Ergodicity Breaking in Coupled Hamiltonian Systems

Rafael M. da Silva[1] · Marcus W. Beims[1] · Cesar Manchein[2]

Received: 13 September 2021 / Accepted: 19 November 2021 / Published online: 6 December 2021

Abstract
Ergodicity breaking has a profound effect on the transport of particles in typical nonlinear Hamiltonian systems. In this paper, we analyze the survival and extinction of ergodicity in weakly chaotic Hamiltonian coupled maps. The key feature for the ergodicity breaking is the existence of sporadic *strong* dynamical trappings (or *strong* quasi-invariant sets in higher dimensions). Such trappings eventually occur when zero Kolmogorov-Sinai-entropy (KSE) is observed along a chaotic trajectory. The finite-time KSE$^{\omega}$ is obtained from the spectrum of finite-time Lyapunov exponents (FTLEs$^{\omega}$) calculated during an arbitrary time window of size ω along the chaotic trajectory. Zero KSE$^{\omega}$ occurs when all FTLEs$^{\omega}$ are sufficiently close to zero, and positive KSE$^{\omega}$ when the sum of the FTLEs$^{\omega}$ is larger than a predefined threshold. The associated points in phase space belong, respectively, to strong and weak quasi-invariant structures. The key observations are that (i) for zero KSE$^{\omega}$, *solely* power-law decays are observed in the cumulative recurrence distribution (characterizing the strong quasi-invariant sets), and (ii) for positive KSE$^{\omega}$ values we obtain asymptotically *only* exponential decays (characterizing the chaotic motion and the weak quasi-invariant sets). For $N = 1, \ldots, 5$ coupled Hamiltonian maps with mixed dynamics, we obtain the power-law decay exponent $\mu \sim 1.20$, which corroborates with former investigations. This result also persists for arbitrarily small coupling strength between the maps. Both outcomes (i) and (ii) are valid for asymptotic times so that our analysis precisely confirms the concept of ergodicity extinction and survival in weakly chaotic systems with a moderate number of dimensions.

Keywords Ergodicity breaking · Hamiltonian systems · Poincaré recurrences · Finite-time Lyapunov exponents.

1 Introduction

For many years, robust results in *equilibrium* statistical mechanics are obtained when time averages can be replaced by spatial averages, a consequence of the ergodic property found in the dynamics of innumerable physical systems. Nevertheless, it has become more and more evident in current researches that in a variety of physical systems, the evolution remains localized for finite times (or transients) [1, 2] in confined areas of the phase space [3]. In the context of nonintegrable Hamiltonian systems with mixed (also defined as divided [4] for systems with two-degrees of freedom) phase space, where regular domains are surrounded by the chaotic sea and define *dynamical trappings* (named as quasi-invariant structures in higher-dimensional phase spaces [5]) or *stickiness*, and can be related to quasi-stationary physical states. Thus, the concept of *ergodicity breaking* is not necessarily restricted to the usual infinite-time scales limit and can be quantified via distinct degrees of stickiness in a physical system. In fact, the goal of this paper is to show that only quasi-invariant sets which affect *all* phase-space dimensions can generate ergodicity breaking. Such sets are referred here as *strong* quasi-invariant sets.

In general, different mechanisms can activate non-ergodicity in distinct contexts and is of most relevance to understand and to explore the origin of this activation.

Rafael M. da Silva and Marcus W. Beims equally contributed to this work.

✉ Cesar Manchein
cesar.manchein@udesc.br

Rafael M. da Silva
rmarques@fisica.ufpr.br

Marcus W. Beims
mbeims@fisica.ufpr.br

[1] Departamento de Física, Universidade Federal do Paraná, Curitiba 81531-980, Paraná, Brazil

[2] Departamento de Física, Universidade do Estado de Santa Catarina, Joinville 89219-710, Santa Catarina, Brazil

The breakdown of the ergodic behavior has important consequences in problems involving condensed matter physics [6, 7], transport properties in classical Hamiltonian systems [3, 8–12] (see also references therein) and in quantum systems that violate the eigenstate thermalization hypothesis [13–16], to mention a few examples. From a practical point of view, a recent study shows that the phenomenon of ergodicity breaking also occurs in biophysical systems, and it has crucial implications in biomedical applications where long observations of time-series are impossible [17]. Another example is found in Ref. [18], where the author addresses the question of how ergodicity may be used to understand the complicated current economic formalism.

Being more specific, in this paper, we show that only *strong* quasi-invariant structures (*strong* dynamical trappings) in the phase space are responsible for the *extinction* of ergodicity. The strong dynamical trappings are observed when the Kolmogorov-Sinai-entropy (KSE) approaches zero for a finite time, along with the evolution of the chaotic trajectory. In other words, ergodicity breaking only occurs when the quasi-regular structures in the phase space *affect simultaneously all* FTLEs$^{\omega}$ related to the unstable invariant manifolds. In case the quasi-regular structures *does not* affect simultaneously all the positive FTLEs$^{\omega}$, defined here as *weak* dynamical trappings, ergodicity survives. In this context, the authors in Ref. [19] also applied the concept of finite-time KS entropy (defined differently) and look at the fluctuations of this quantity in an ensemble of trajectories as a potential measure that can indicate the ergodicity breaking in high-dimensional Hamiltonian systems.

The paper is organized as follows. In Sect. 2, the model of together with some numerical simulations, Hamiltonian coupled maps are presented to exhibit the dynamics in phase space of a single map using distinct nonlinear parameter values. This furnishes a better understanding of the dynamics when the maps are coupled. Section 3 presents the definition of the KSE$^{\omega}$ together with a numerical example for the case of two coupled maps. In Sect. 4, results for the cumulative distributions of the consecutive times spent inside the quasi-invariant structures are presented, compared and discussed for the coupled maps case. Finally, in Sect. 5 we summarize our main findings.

2 Coupled Maps Model

Coupled symplectic maps are convenient systems to investigate the ergodicity breaking in high-dimensional phase space of Hamiltonian systems. In this study, we used a $2N$-dimensional symplectic mapping composed of N copies of the well-known Chirikov-Taylor standard map [20] (see also [21]). Such symplectic mapping was previously studied in Refs. [9, 22, 23], and is defined in the following form:

$$\begin{cases} p_i' = p_i + K_i \sin(2\pi x_i) + f(x_{i+1}, x_i, x_{i-1}), \\ x_i' = x_i + p_i', \end{cases} \tag{1}$$

where $K_i \sin(2\pi x_i)$ represents the local conservative nonlinear forcing. The function $f(x_{i+1}, x_i, x_{i-1})$ represents the conservative nonlinear coupling which is defined as

$$f(x_{i+1}, x_i, x_{i-1}) = \beta[\sin(\delta x_+) + \sin(\delta x_-)], \tag{2}$$

with $\delta x_{\pm} = 2\pi(x_{i\pm1} - x_i)$, and β being the coupling strength. Note that the primes in x_i' and p_i' indicate the one-step time evolution of x_i and p_i, respectively, with the index i labelling the map.

In our simulations, we considered periodic boundary conditions $x_i(\text{mod } 1)$ and $p_i(\text{mod } 1)$ with $-0.5 \le p_i \le 0.5$. In the limit of vanishing coupling, $\beta \to 0$, the system (1), reduces to a set of N uncoupled maps, whose phase space exhibits regular, chaotic, or mixed dynamics, depending on the value of the nonlinear parameters K_i. The underlying symplectic (Hamiltonian) flow that originates the generic lattice of N coupled mappings (1) describes the dynamics of the N single kicked rotors interacting through a nearest-neighbor coupling force. For $N = 2$ the coupled maps lattice studied here is very similar to the Froeschlé map introduced in [24] and used to model the time evolution of elliptical galaxies.

We study the dynamics of $N = 2$, 3, and 5 coupled standard maps, whose phase-space dimension is 4, 6 and 10, respectively. For the coupling strength, we used $\beta = 10^{-4}$, 10^{-3}, and 10^{-2}, and five kicking intensities: $(K_1, K_2, K_3, K_4, K_5) = (0.23, 0.41, 0.42, 0.81, 1.40)$. The first four values of K_i correspond to a mixed-phase space composed of chaotic sea and chains of regular islands [21] (see Fig. 1), known as sticky domains. The *stickiness effect* yields asymptotic algebraic decay of Poincaré recurrences, and in these cases, ergodicity can be broken. We point out that some dynamical properties of (1) have been studied in Refs. [9, 22, 23]. In particular, the simulations in [22] indicate that a coarse-grained filling of the phase space (typical behavior of the ergodic systems) is obtained even for small nonlinearity parameters ($\beta \le 10^{-4}$), while the mixed nature of the phase space can make this filling extremely slow, compatible with power-law scaling. In [23], fluctuations of FTLEs were considered, suggesting a relationship between fluctuations and sticking to regular orbits.

Figure 1 displays the phase-space dynamics of one uncoupled map for increasing values of K. In Fig. 1(a) to (c), a mixed dynamics due to divided phase spaces is shown with several isolated islands surrounded by high-order resonances and a chaotic component. While in Fig. 1(d) some small islands are still present, Fig. 1(e) suggests full chaotic dynamics.

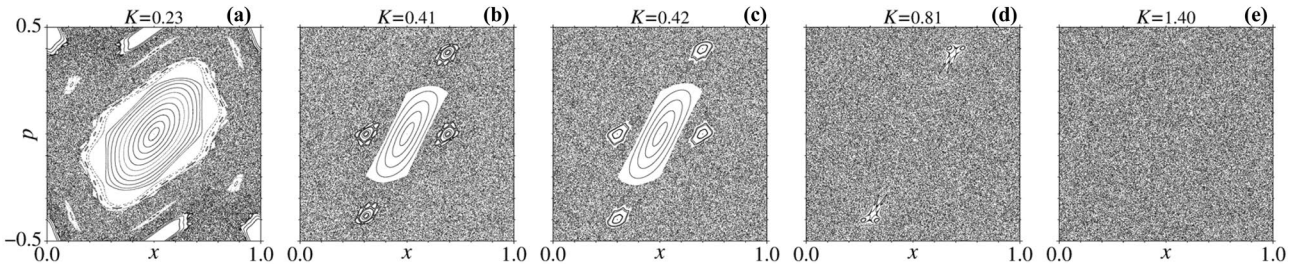

Fig. 1 Phase-space dynamics of the uncoupled $\beta = 0$ standard map for (**a**) $K = 0.23$, (**b**) $K = 0.41$, (**c**) $K = 0.42$, (**d**) $K = 0.81$, and (**e**) $K = 1.40$. These values of K are also used in the nonzero coupling numerical simulations. Here we used 120 equally distributed initial conditions. Each initial condition was iterated 5000 times

3 The KSE$^{\omega}$ and the Quasi-invariant Sets

A typical chaotic trajectory visits all points in the phase space of high-dimensional mixed Hamiltonian systems. Let $\{\mathbf{x}\} \in \Gamma$ the set of points of such chaotic trajectory and $\Gamma = \Gamma_{\text{chaos}}$ the phase space. For asymptotic times ($t \to \infty$) in a closed Hamiltonian system with N degrees of freedom, the chaotic trajectory can be characterized by a spectrum of N positive Lyapunov exponents $\{\lambda^{(\infty)}_{i=1\ldots 2N}\}$, where $\lambda^{(\infty)}_1 > \lambda^{(\infty)}_2, \ldots, \lambda^{(\infty)}_N > 0 > -\lambda^{(\infty)}_N >, \ldots, -\lambda^{(\infty)}_2 > -\lambda^{(\infty)}_1$. Even though the spectrum of FTLEs is a powerful method to describe the underline dynamics, unfortunately, the effect of quasi-invariant sets on the chaotic trajectory in mixed-phase spaces is washed out for asymptotic times. To solve this problem, a time-dependent spectrum $\{\lambda^{(\omega)}_{i=1\ldots 2N}(t)\}$ can be used, and is obtained when the spectrum of FTLEs is computed along the chaotic trajectory during a window of size ω. More interestingly, it has been shown [25] that sharp transitions towards $\lambda^{(\omega)}_i \approx 0$ occur when the chaotic trajectory approaches regular islands (or the quasi-regular structures). Such sharp transitions towards zero of one or more $\lambda^{(\omega)}_i$ are related to points in phase space that belong to quasi-invariant structures. Therefore, the chaotic component of the phase space can be divided in sub-components

$$\Gamma_{\text{chaos}} = \Gamma^{(\omega)}_{\text{chaos}} + \sum_{n=1}^{N} \Gamma^{(2n)}_{\text{quasi}}, \tag{3}$$

$\Gamma^{(\omega)}_{\text{chaos}}$ represents the chaotic phase space sub-component for which all $\lambda^{(\omega)}_i > 0$. On the other hand, $\Gamma^{(2n)}_{\text{quasi}}$ represents the distinct quasi-invariant sub-components which have a number $2n$ of $\lambda^{(\omega)}_i$ which are *simultaneously* close to zero. Each sub-component $\Gamma^{(2n)}_{\text{quasi}}$ is related to points in phase space which belong to quasi-invariant structures. Figure 2 displays these sub-components in a time series of system (1) with $N = 2$.

To study ergodicity breaking process through quasi-invariant structures, it is appropriate to define the KSE, which according to Pesin [26] (see also [27]) is equal to the sum of the positive Lyapunov exponents for times large enough. Using the time-dependent spectrum of positive $\{\lambda^{(\omega)}_{i=1\ldots N}\}$, it is possible to define the finite-time KSE$^{\omega}$ inside a time window ω as

$$\text{KSE}^{\omega} = \sum_{i=1}^{N} \lambda^{(\omega)}_i. \tag{4}$$

Consequently, the KSE$^{\omega}$ changes along the chaotic trajectory, depending on which quasi-invariant structure is visited. When all $\{\lambda^{(\omega)}_{i=1\ldots N}\}$ approach zero simultaneously, the KSE$^{\omega}$ also approaches zero and we have the already mentioned *strong quasi-invariant structures*. The term strong refers to the ability of the structure to affect simultaneously all $\{\lambda^{(\omega)}_{i=1\ldots N}\}$. As demonstrated later, only the strong quasi-invariant structures, for which $n = N$, are capable to break the ergodicity.

For the practical determination of the sub-components $\Gamma^{(2n)}_{\text{quasi}}$, it is necessary to settle a threshold for the FTLEs $\lambda^{(\omega)}_i$

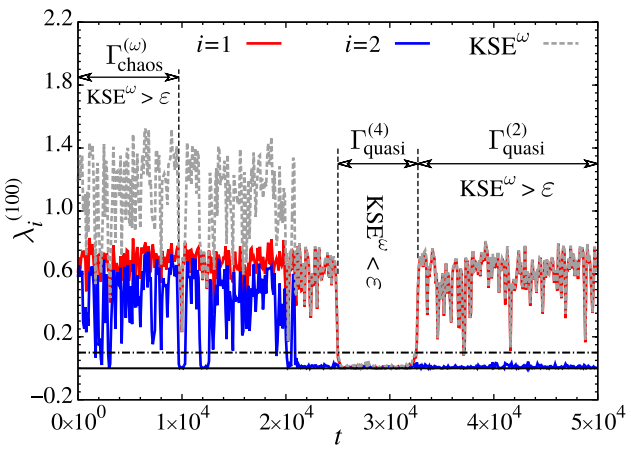

Fig. 2 Time series of the FTLEs $\lambda^{(\omega)}_i$ ($i = 1, 2$) for the system (1) with $K_1 = 0.41$, $K_2 = 0.42$, and $\beta = 10^{-3}$, showing the time intervals for which the chaotic sub-component $\Gamma^{(\omega)}_{\text{chaos}}$ and quasi-invariant sub-components $\Gamma^{(2)}_{\text{quasi}}$ and $\Gamma^{(4)}_{\text{quasi}}$ are visited. The threshold $\varepsilon = \varepsilon_1 + \varepsilon_2 = 0.10$ is represented by the black dash-dotted line, while the black continuous line indicates the zero value

so that $\mathrm{KSE}^{\omega} < \varepsilon$, with $\varepsilon = \sum_{i=1}^{N} \varepsilon_i$. Additionally, the choice of a few parameters and conventions are needed. First of all, the window size ω and the threshold ε_i directly affects the recognition of the quasi-invariant sets. They can be interpreted as the phase-space resolution of the analysis and should be selected to provide maximal information about the regions of interest. The window size ω must be satisfactory small to assure an acceptable resolution of the temporal changes of the $\lambda_i^{(\omega)}$'s, but also sufficiently large to have a reliable estimation (see Refs. [22, 28]). Another important choice is the method for the computation of the FTLEs. We used Benettin's algorithm [29, 30], which includes the Gram-Schmidt re-orthonormalization procedure. The decreasing order of $\lambda_i^{(\omega)}$ is valid on average, but inversions of the order ($\lambda_{i+1}^{(\omega)} > \lambda_i^{(\omega)}$) may occur for some times t and we have chosen to establish the order of $\lambda_i^{(\omega)}$ for all t. At last, it is possible to determine how to sample the time series $\lambda_i^{(\omega)}$. While the FTLEs are determined for all t, there is a correlation between the values of FTLEs inside a window of size ω, since they are computed using the same points of the trajectory. In order to avoid this trivial correlation the series of $\lambda_i^{(\omega)}$ can be computed using non-overlapping windows, *i.e.* plotting $\lambda_i^{(\omega)}$ only every ω time steps (a choice we adopt in our simulations). The probability density function of $\lambda_i^{(\omega)}$ has been extensively studied [23, 28, 31].

Finally, considering high-dimensional Hamiltonian systems, it seems more appropriated to study a finite-time KSE and to analyze the variations of this quantity in an ensemble of trajectories as a potential measure that indicates the break of ergodicity which occurs due to the intermittent stickiness synchronization observed for such class of dynamical systems [32, 33].

4 Results and Discussion

In order to provide a clear presentation of the results, we start discussing the time dependence of KSE^{ω} along the chaotic trajectory and the cumulative distribution of the consecutive times τ_{KSE} spent inside each quasi-invariant structures for $N = 2$. Later on we discuss the cumulative distribution of τ_{KSE} in cases $N = 3$ and 5 for the full quasi-invariant structures.

Figure 3(a)–(d) show the log-log plot of the cumulative recurrence distribution $P_{\mathrm{cum}}(\tau)$ as a function of the consecutive time τ spent inside each quasi-invariant structures for distinct combination of K_1 and K_2 from the two coupled map system (1). In this case the phase space dimension is $N = 4$. Table 1 summarizes the combination of K_1 and K_2 parameters and the thresholds used in each case. We consider different nonlinearity parameters in order to characterize the influence of (i) breaking the regular islands symmetry between maps and (ii) suppressing the regular islands in phase space of the uncoupled maps and for the dynamics of the whole multidimensional system. In this way, the maps of the lattice have different ergodic properties and transport rates, which the combined effect is explored in the present study. Different colors represent the cumulative recurrence distribution of the distinct quasi-invariant structures: $\Gamma^{(\omega)}_{\mathrm{chaos}}$ in orange, $\Gamma^{(2)}_{\mathrm{quasi}}$ in dark blue and $\Gamma^{(4)}_{\mathrm{quasi}}$ in cyan. While the distributions related to $\Gamma^{(\omega)}_{\mathrm{chaos}}$ and $\Gamma^{(2)}_{\mathrm{quasi}}$ decay exponentially, for the strong quasi-invariant structure $\Gamma^{(4)}_{\mathrm{quasi}}$ a power-law decay is observed. The power-law decay exponent γ tends to increase when one of the coupled maps has a larger value of the nonlinear parameter, as exemplified in Fig. 3(c) for which $K_2 = 0.81$. Similar power-law decays are also observed for the statistics of the Poincaré recurrence times in high-dimensional coupled maps [34–37] and in non-Hamiltonian conservative systems [38]. Albeit these works, the generic mechanism that could explain these power-law decays remains an open question [39, 40]. In contrast to the high-dimensional case, the power-law decay for the recurrence times (with $\gamma \sim 1.57$) in two-dimensional maps [31, 41–48] is well-known, and it occurs due to the hierarchy islands-around-islands in the phase space [49]. In the case for which $K_2 = 1.40$ [see Fig. 1(e)], the chaotic component $\Gamma^{(\omega)}_{\mathrm{chaos}}$ dominates the phase space and eliminates any contribution of the strong quasi-invariant structure, as can be checked by the absence of the $\Gamma^{(4)}_{\mathrm{quasi}}$ case in Fig. 3(d).

Figure 3(e)–(h) display the $x_2 \times p_2$ phase-space projections with colors indicating the points in phase space which belong to the corresponding quasi-invariant structures from Fig. 3(a)–(d). The relation to the corresponding cyan, dark blue, and orange points from Fig. 3(e)–(h) is evident. The full quasi-invariant structures are clearly related to points in phase space which correspond to sticky motion (see cyan points). For a better visualization, Fig. 3(i)–(l) display the points in phase space (brown color) solely related to the full quasi-invariant structures for which $\mathrm{KSE}^{\omega} < \varepsilon$. Thus, the power-law decay from Fig. 3(a)–(c) are a consequence of the brown points in Fig. 3(i)–(k), respectively. Furthermore, the absence of such points in Fig. 3(l) leads to the extinction of any power-law decay in Fig. 3(d).

This result is remarkable since it shows that only states along with the chaotic trajectory with zero ($< \varepsilon$) KSE^{ω} can generate stickiness and non-ergodic motion. We point out that a similar power-law exponent γ was obtained for the same system by using both, statistics of Poincaré recurrences and large deviations for the distribution of FTLEs [9]. The fundamental ingredient for the power-law decay is the coupling force between maps. Even for arbitrarily small couplings (as used here), chaotic trajectories penetrate and remain trapped in the reminiscence of high-order resonance islands for long, but finite intervals, which drastically

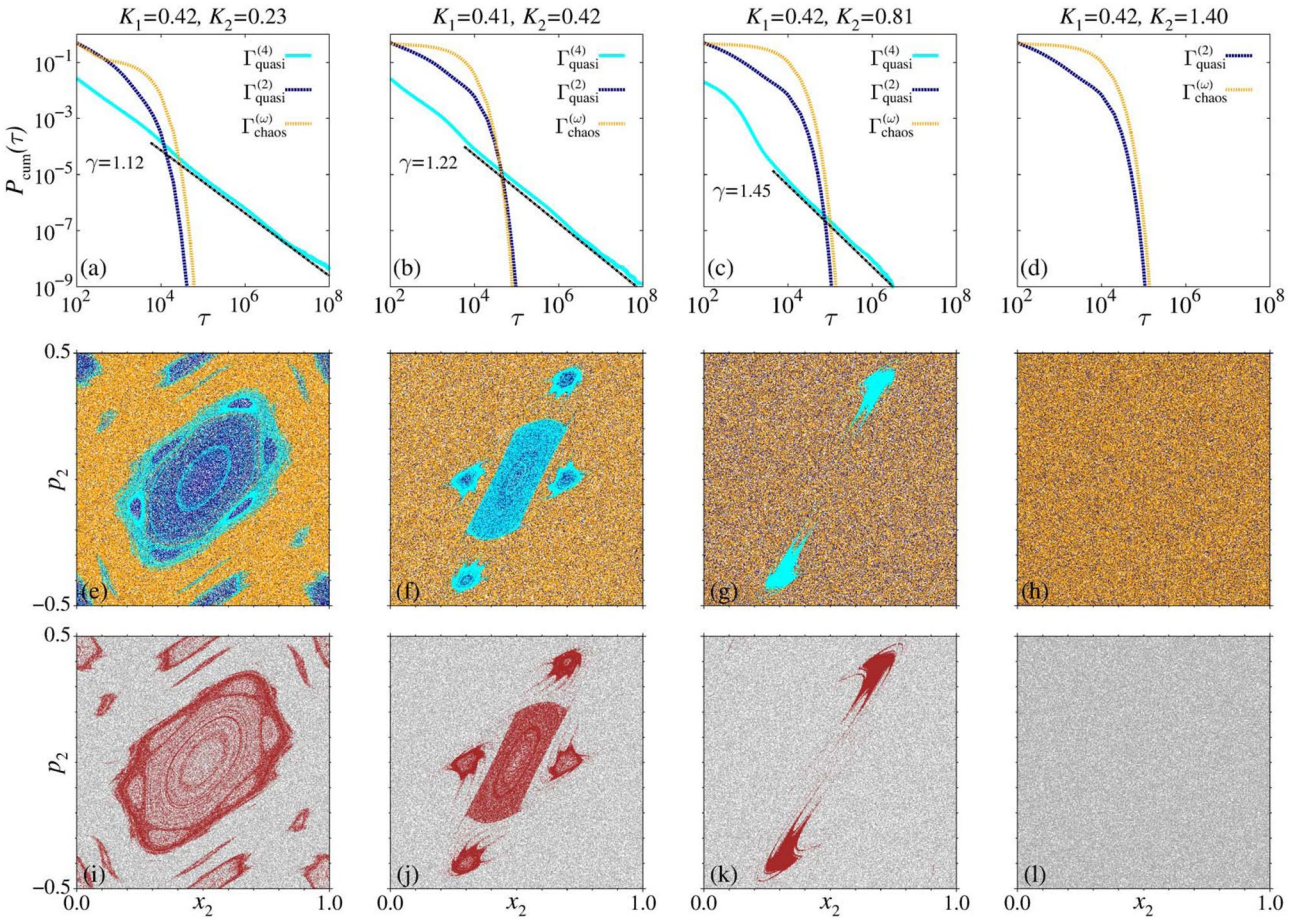

Fig. 3 (**a**)–(**d**) The cumulative distribution $P_{cum}(\tau)$ of the consecutive times τ inside the quasi-invariant structures $\Gamma^{(2)}_{quasi}$ and $\Gamma^{(4)}_{quasi}$, and the chaotic sub-component $\Gamma^{(\omega)}_{chaos}$, obtained during a time window $\omega = 100$ for system (1) with $N = 2$, $\beta = 10^{-3}$, and different values of K_i. The thresholds ε_i are approximately equal to 10% of the value of $\lambda_i^{(\infty)}$ (see Table 1). The distributions were performed collecting 10^{10} values of τ, and the $\Gamma^{(4)}_{quasi}$ sub-component follows a power-law decay with exponent γ. In (**e**)–(**h**) the phase-space projections $x_2 \times p_2$ are displayed with the colors indicating the points in the phase space corresponding to (**a**)–(**d**), while in (**i**)–(**l**) the colors indicate the corresponding phase space points related to KSE^{ω}, which are brown points for $KSE^{\omega} < \varepsilon$, and gray points for $KSE^{\omega} > \varepsilon$, with $\varepsilon = \varepsilon_1 + \varepsilon_2$

degrades the chaotic dynamics. In particular, the coupling force acts mainly in the tangential directions as a kind of random signal (see Refs. [50, 51] for enlightening discussions). Such phenomenon generates the trapping of the chaotic trajectories and it is responsible for long transients in the power-law decay of $P_{cum}(\tau)$, and consequently also responsible for the non-ergodic motion, even when the coupling strength is varied and the system contains many coupled particles. This scenario is clarified by the numerical results which are presented next.

Table 1 Values of K_i used to couple two standard maps ($N = 2$) and the thresholds ε_i and $\varepsilon = \varepsilon_1 + \varepsilon_2$. For $N = 2$ we set $\varepsilon_i \sim 10\%$ of the value of $\lambda_i^{(\infty)}$. Associated Fig. 3 are indicated

Figure 3	K_1, K_2	ε_1	ε_2	ε
(a), (e), (i)	0.42, 0.23	0.05	0.02	0.07
(b), (f), (j)	0.41, 0.42	0.06	0.04	0.10
(c), (g), (k)	0.42, 0.81	0.10	0.05	0.15
(d), (h), (l)	0.42, 1.40	0.15	0.05	0.20

Figure 4(a) displays the cumulative distribution of the consecutive times τ_{KSE} for $P_{cum}(\tau_{KSE<\varepsilon})$ (gray dotted curve) and $P_{cum}(\tau_{KSE>\varepsilon})$ (brown curve). While the gray dotted curve decays exponentially, the brown curve decays as a power-law function

$$P_{cum}(\tau_{KSE}) \propto a\tau_{KSE}^{\mu}, \tag{5}$$

with exponent $\mu = 1.25$. The black dotted line shows the decay $\mu = 1.25$ for reference. This result demonstrates that only the distribution $P_{cum}(\tau_{KSE<\varepsilon})$, which is uniquely related to the strong invariant sets, is responsible for the extinction of ergodicity. The robustness of these findings under variations of the thresholds ε and windows ω are shown in Fig. 4. While in Fig. 4(b) we see the cumulative distribution $P_{cum}(\tau_{KSE<\varepsilon})$

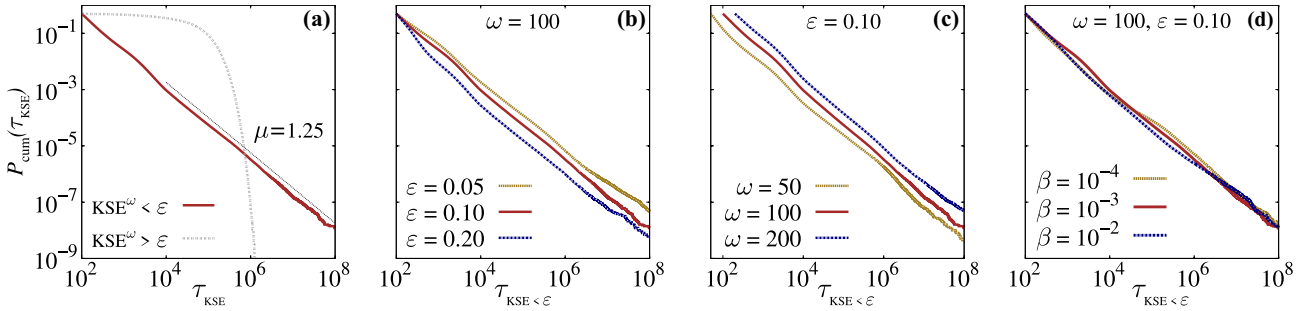

Fig. 4 The cumulative distribution $P_{cum}(\tau_{KSE})$ of the consecutive times τ_{KSE} in (**a**) for $P_{cum}(\tau_{KSE<\varepsilon})$ (brown curve) and $P_{cum}(\tau_{KSE>\varepsilon})$ (gray dotted curve) for the time window $\omega = 100$ for system (1) with $N = 2$, $\beta = 10^{-3}$, $K_1 = 0.41$, and $K_2 = 0.42$. The threshold $\varepsilon = 0.10$ is approximately equal to 10% of the value of $\lambda_1^{(\infty)} + \lambda_2^{(\infty)}$. The distribution performed collecting 10^9 values of τ_{KSE}, and $P_{cum}(\tau_{KSE<\varepsilon})$ follows a power-law decay with exponent $\mu = 1.25$ (see dotted black line for reference). The cumulative distribution $P_{cum}(\tau_{KSE<\varepsilon})$ is shown in (**b**), where we kept fixed the time window $\omega = 100$ and varied the threshold ε chosen values about 5%, 10% and 20%, while in (**c**), the threshold $\varepsilon = 0.10$ was kept fixed and the time window ω was varied. In (**d**) the cumulative distribution is shown for distinct values of the coupling parameter β, for $\omega = 100$ and $\varepsilon = 0.10$

for a fixed value of the time window $\omega = 100$ and three distinct thresholds $\varepsilon = 0.05, 0.10, 0.20$, in Fig. 4(c) we display the distribution for a fixed threshold $\varepsilon = 0.10$ and three different time windows $\omega = 50, 100, 200$. For reference, the brown curve repeats the result from Fig. 4(a). This means that the values of the window ω and thresholds ε used here allow us to make trustful statements. Additionally, Fig. 4(d) presents results for $P_{cum}(\tau_{KSE<\varepsilon})$ for distinct values of the coupling parameter, namely $\beta = 10^{-2}, 10^{-3}$ and 10^{-4}. The persistence of the power-law decay with $\mu = 1.25$ is visible.

Finally we discuss results for higher dimensions. Figure 5 shows the same cumulative distribution $P_{cum}(\tau_{KSE<\varepsilon})$ for $N = 2, 3$ and $N = 5$, keeping fixed $\beta = 10^{-3}$. Table 2 summarizes the values of K_i and thresholds used in Fig. 5. In all cases, the power-law decay is evident and it follows an exponent $\mu \sim 1.25$ obtained for the $N = 2$ case (see Fig. 4), which is consistent with former results [9] where the exponent which characterizes the stickiness effect was estimated by different statistical analysis for $N = 2,\ 3$ coupled maps (1). Besides, it allows us to reaffirm that strong quasi-invariant structures are uniquely related to non-ergodic portions of the phase space. It is also important to mention that the estimated value of μ partially agree with Shepelyansky's conjecture, which, roughly speaking, proposes the existence of an asymptotic decay of Poincaré recurrences for coupled Hamiltonian maps with arbitrary number of degrees of freedom. However, the average decay exponent obtained here ($\mu \sim 1.20$) is smaller than the universal average decay Poincaré exponent between ~ 1.3 and 1.4 originally proposed in [37].

Above results demonstrate that $P_{cum}(\tau_{KSE>\varepsilon})$ excludes the effect of quasi-invariant sets on the ergodicity breaking. Thus, weak quasi-invariant structures are not able to generate the survival of ergodicity. In other words, any quasi-invariant structure with at least one positive $\lambda_i^{(\omega)}$ is capable of generating ergodicity. On the other hand, $P_{cum}(\tau_{KSE<\varepsilon})$, related to strong quasi-invariant sets leads to the extinction of ergodicity.

Furthermore, considering that each point along the chaotic trajectory belongs to a point in phase space, all points which belong to the KSE$^{\omega} < \varepsilon$ generate a pure power-law decay of $P_{cum}(\tau_{KSE<\varepsilon})$ which for large times (observed in the simulations) never reach an exponential decay. Thus, if we consider only the portion of points in phase space and times which belong to zero KSE$^{\omega} < \varepsilon$ [brown points in Figs. 3(i)–(k)], we can identify the regions in phase space which generate the ergodicity breaking, valid for asymptotic times.

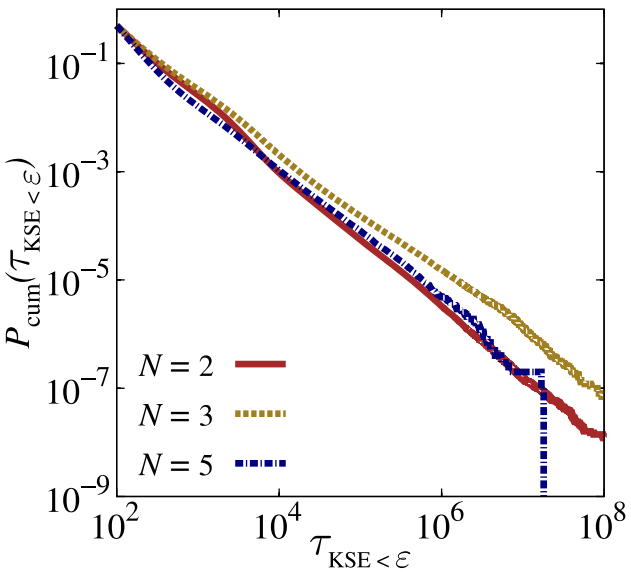

Fig. 5 The cumulative distribution $P_{cum}(\tau_{KSE<\varepsilon})$ of the consecutive times $\tau_{KSE<\varepsilon}$ in the regime KSE$^{\omega} < \varepsilon$ (for $\omega = 100$) obtained for system (1). We used different values of N and K_i according to Table 2, for $\beta = 10^{-3}$. The brown continuous curve is the same curve from Fig. 4, which follows a power-law decay with exponent $\mu = 1.25$

Table 2 Values of K_i used to couple the standard maps and the threshold ε. For $N = 2$ we set $\varepsilon \sim 10\%$ of the value of $\sum_{i=1}^{N} \lambda_i^{(\infty)}$, while for $N = 3$ and $N = 5$ $\varepsilon \sim 5\%$ of this sum

Value of K_i/ε	$N = 2$	$N = 3$	$N = 5$
K_1	0.41	0.41	0.41
K_2	0.42	0.42	0.42
K_3	-	0.43	0.43
K_4	-	-	0.44
K_5	-	-	0.45
ε	0.10	0.08	0.15

5 Conclusions

The breakdown of the ergodic behavior in realistic physical systems has received abundant attention in recent years [6, 7, 9, 11, 13–17]. The anomalous diffusion process found in weakly chaotic Hamiltonian systems results from the sticky motion, generating the ergodicity breaking. The power-law decay can characterize sticky motion of the cumulative recurrence distribution of specific physical quantities. It has been shown recently [34] that the concept of order, semi-ordered and chaotic regimes of motion [25, 52] can be used to improve the characterization of the sticky motion significantly.

Based on the concept of quasi-invariant sets in mixed chaotic Hamiltonian systems and the determination of the finite-time Lyapunov exponents (FTLE$^{\omega}$), in this paper, we use the zero and positive finite-time Kolmogorov-Sinai entropy (KSE$^{\omega}$) to explain the survival and extinction of ergodicity in such systems. The KSE$^{\omega}$ are obtained from the spectrum of FTLEs calculated during a time window of size ω along the chaotic trajectory. We studied the cases of $N = 2,\ 3$ and 5 coupled Chirikov-Taylor standard maps and the results were shown to be robust under the changes of the time window ω, thresholds ε, and coupling strengths β between the standard maps with different nonlinearity parameters K_i. The main observation was that only points in phase space with zero KSE$^{\omega}$ induce power-law decays in the cumulative recurrence distribution. Such points are related to *strong* quasi-invariant sets, since they are capable of driving FTLEs$^{\omega}$ simultaneously close to zero, leading to a region in phase-space which is free of ergodicity. Therefore, we demonstrate that inside such region the extinction of ergodicity occurs. On the other hand, all quasi-invariant sets related to positive KSE$^{\omega}$, *only* induce exponential decays in the cumulative recurrence distributions. These are named as *weak* quasi-invariant sets. This means that ergodicity breaking in weakly chaotic Hamiltonian coupled maps is only possible when strong quasi-invariant sets exist along a chaotic trajectory. This is valid for asymptotic times so that our proposal precisely confirms the concept of ergodicity breaking in weakly chaotic systems. Ergodicity survives in the presence of weak quasi-invariant sets, for which at least one FTLE$^{\omega}$ is larger than zero.

As high-dimensional Hamiltonian systems (with mixed phase space) share the fundamental property that resonance islands are no more forbidden regions in phase space, the ergodicity breaking is only possible when zero KSE$^{\omega}$ exist along a chaotic trajectory, and it might be extended to even higher-dimensional systems ($N > 5$). Remains also the question if dynamical systems, in general, always allow such strong quasi-invariant sets. Two interesting byproducts of the analysis of the cumulative distribution $P_{\text{cum}}(\tau_{\text{KSE}<\varepsilon})$ regimes of motion are the following: (i) the possibility of visualizing projections of the phase space that highlight the topological structures responsible for the large return times (it would be interesting a direct comparison of quasi-invariant sets obtained via KSE$^{\omega}$ and those obtained through the more complicated algorithms used in [53]); and (ii) the decay of $P_{\text{cum}}(\tau_{\text{KSE}<\varepsilon})$ can be used to estimate the correlations decay in systems with mixed phase space composed by a moderate number of degrees of freedom.

Acknowledgements The authors thank the National Council for Scientific and Technological Development – CNPq (Brazilian agency) for financial support (Grant Numbers 432029/2016-8, 310792/2018-5, 424803/2018-6, and 310228/2020-4), and they also acknowledge computational support from Prof. C. M. de Carvalho at LFTC-DFis-UFPR (Brazil). C. M. also thanks FAPESC (Brazilian agency) for financial support.

Data Availability The data that support the findings of this study are available from the corresponding author upon reasonable request.

Declarations

Conflicts of Interest The authors declare that they have no known competing financial interests or personal relationships that could have appeared to influence the work reported in this paper.

References

1. J.D.V. Hermes, E.D. Leonel, Characteristic times for the Fermi-Ulam model. Int. J. Bifurcation Chaos **31**(02), 2130004 (2021)
2. V.M. Rothos, C. Antonopoulos, L. Drossos, Chaos in a near-integrable Hamiltonian lattice. Int. J. Bifurcation Chaos **12**(08), 1743–1754 (2002)
3. P. Gaspard, *Chaos Scattering and Statistical Mechanics* (Cambridge University Press, Cambridge, 1998)
4. B.V. Chirikov, Chaotic dynamics in Hamiltonian systems with divided phase space, in *Dynamical System and Chaos*. ed. by L. Garrido (Springer, Berlin, Heidelberg, 1983), pp. 29–46
5. G. Froyland, K. Padberg, Almost-invariant sets and invariant manifolds – connecting probabilistic and geometric descriptions of coherent structures in flows. Physica D **238**, 1507 (2009)
6. G. Gradenigo, F. Antenucci, L. Leuzzi, Glassiness and lack of equipartition in random lasers: The common roots of ergodicity breaking in disordered and nonlinear systems. Phys. Rev. Research **2**, 023399 (2020)

7. T. Mori, T.N. Ikeda, E. Kaminishi, M. Ueda, Thermalization and prethermalization in isolated quantum systems: A theoretical overview. J. Phys. B At. Mol. Opt. Phys. **51**, 112001 (2018)
8. M. Falcioni, U.M.B. Marconi, A. Vulpiani, Ergodic properties of high-dimensional symplectic maps. Phys. Rev. A **44**, 2263 (1991)
9. T.M. Oliveira, R. Artuso, C. Manchein, Collapse of hierarchical phase space and mixing rates in Hamiltonian systems. Physica A **530**, 121568 (2019)
10. C. Manchein, M.W. Beims, J.M. Rost, Characterizing the dynamics of higher dimensional nonintegrable conservative systems. Chaos **22**, 033137 (2012)
11. M.W. Beims, C. Manchein, J.M. Rost, Origin of chaos in soft interactions and signatures of nonergodicity. Phys. Rev. E **76**, 056203 (2007)
12. G. Radons, Weak ergodicity breaking and aging of chaotic transport in Hamiltonian systems. Phys. Rev. Lett. **113**, 184101 (2014)
13. S. Roy, A. Lazarides, Strong ergodicity breaking due to local constraints in a quantum system. Phys. Rev. Research **2**, 023159 (2020)
14. J.M. Deutsch, Eigenstate thermalization hypothesis. Rep. Prog. Phys. **81**(8), 082001 (2018)
15. L. D'Alessio, Y. Kafri, A. Polkovnikov, M. Rigol, From quantum chaos and eigenstate thermalization to statistical mechanics and thermodynamics. Adv. Phys. **65**(3), 239–362 (2016)
16. J. Eisert, M. Friesdorf, C. Gogolin, Quantum many-body systems out of equilibrium. Nature Phys. **11**, 124 (2015)
17. M. Nosonovsky, P. Roy, Allometric scaling law and ergodicity breaking in the vascular system. Microfluid. Nanofluid. **24**, 53 (2020)
18. O. Peters, The ergodicity problem in economics. Nat. Phys. **15**, 1216 (2019)
19. A. Lakshminarayan, S. Tomsovic, Kolmogorov-Sinai entropy of many-body Hamiltonian systems. Phys. Rev. E **84**, 016218 (2011)
20. B.V. Chirikov, A universal instability of many-dimensional oscillator systems. Phys. Rep. **52**, 263 (1979)
21. A.J. Lichtenberg, M.A. Lieberman, *Regular and Chaotic Dynamics* (Springer, New York, 1992)
22. H. Kantz, P. Grassberger, Chaos in low-dimensional Hamiltonian maps. Phys. Lett. A **123**, 437 (1987)
23. H. Kantz, P. Grassberger, Internal Arnold diffusion and chaos thresholds in coupled symplectic maps. J. Phys. A: Math. Gen. **21**, 127 (1988)
24. C. Froeschlé, Numerical study of a four dimensional mapping. Astron. Astrophys. **16**, 172–189 (1972)
25. A. Malagoli, G. Paladin, A. Vulpiani, Transition to stochasticity in Hamiltonian systems: Some numerical results. Phys. Rev. A **34**, 1550–1555 (1986)
26. Y. Pesin, Characteristic Lyapunov exponents and smooth ergodic theory. Russ. Math. Surv. **32**, 55 (1977)
27. J. Eckmann, D. Ruelle, Ergodic theory of chaos and strange attractors. Rev. Mod. Phys. **57**, 617 (1985)
28. J.D. Szezech, S.R. Lopes, R.L. Viana, Finite-time Lyapunov spectrum for chaotic orbits of non-integrable Hamiltonian systems. Phys. Lett. A **335**, 394–401 (2005)
29. G. Benettin, L. Galgani, A. Giorgilli, J.-M. Strelcyn, Lyapunov characteristic exponents for smooth dynamical systems and for Hamiltonian systems: A method for computing all of them. Part 1: Theory. Meccanica **15**(1), 09 (1980)
30. A. Wolf, J.B. Swift, H.L. Swinney, J.A. Vastano, Determining Lyapunov exponents from a time series. Physica D **16**(3), 285–317 (1985)
31. R. Artuso, C. Manchein, Instability statistics and mixing rates. Phys. Rev. E **80**, 036210 (2009)
32. K. Kaneko, R.J. Bagley, Arnold diffusion, ergodicity and intermittency in a coupled standard mapping. Phys. Lett. A **110**(9), 435–440 (1985)
33. R.M. da Silva, C. Manchein, M.W. Beims, Intermittent stickiness synchronization. Phys. Rev. E **99**, 052208 (2019)
34. R.M. da Silva, C. Manchein, M.W. Beims, E.G. Altmann, Characterizing weak chaos using time series of Lyapunov exponents. Phys. Rev. E **91**, 062907 (2015)
35. M. Ding, T. Bountis, E. Ott, Algebraic escape in higher dimensional Hamiltonian systems. Phys. Lett. A **151**, 395 (1990)
36. E.G. Altmann, H. Kantz, Hypothesis of strong chaos and anomalous diffusion in coupled symplectic maps. Europhys. Lett. **78**, 10008 (2007)
37. D.L. Shepelyansky, Poincaré recurrences in Hamiltonian systems with a few degrees of freedom. Phys. Rev. E **82**, 055202 (2010)
38. R.M. da Silva, M.W. Beims, C. Manchein, Recurrence-time statistics in non-Hamiltonian volume-preserving maps and flows. Phys. Rev. E **92**, 022921 (2015)
39. S. Lange, A. Bäcker, R. Ketzmerick, What is the mechanism of power-law distributed Poincaré recurrences in higher-dimensional systems? Eur. Phys. Lett **30002**, 116 (2016)
40. S. Lange, M. Richter, F. Onken, A. Bäcker, R. Ketzmerick, Global structure of regular tori in a generic 4D symplectic map. Chaos **024409**, 24 (2014)
41. C.F.F. Karney, Long-time correlations in the stochastic regime. Physica D **8**, 360 (1983)
42. B.V. Chirikov, D.L. Shepelyansky, Correlation properties of dynamical chaos in Hamiltonian systems. Physica D **13**, 395 (1984)
43. R.S. MacKay, J.D. Meiss, I.C. Percival, Transport in Hamiltonian systems. Physica D **13**, 55 (1984)
44. J.D. Meiss, E. Ott, Markov-Tree model of intrinsic transport in Hamiltonian systems. Phys. Rev. Lett. **55**(25), 2741 (1985)
45. V. Rom-Kedar, S. Wiggins, Transport in two-dimensional maps. Arch. Rational Mech. Anal. **109**, 239 (1990)
46. G.M. Zaslavsky, Dynamical traps. Physica D **168–169**, 292 (2002)
47. G. Cristadoro, R. Ketzmerick, Universality of algebraic decays in Hamiltonian systems. Phys. Rev. Lett. **100**, 184101 (2008)
48. E.G. Altmann, T. Tél, Poincaré recurrences from the perspective of transient chaos. Phys. Rev. Lett. **100**, 174101 (2008)
49. O. Alus, S. Fishman, J.D. Meiss, Statistics of the island-around-island hierarchy in Hamiltonian phase space. Phys. Rev. E **90**, 062923 (2014)
50. C.S. Rodrigues, A.P.S. de Moura, C. Grebogi, Random fluctuation leads to forbidden escape of particles. Phys. Rev. E **82**, 026211 (2010)
51. A. Kruscha, R. Ketzmerick, H. Kantz, Biased diffusion inside regular islands under random symplectic perturbations. Phys. Rev. E **85**, 066210 (2012)
52. G. Contopoulos, L. Galgani, A. Giorgilli, On the number of isolating integrals in Hamiltonian systems. Phys. Rev. A **18**, 1183–1189 (1978)
53. G. Froyland, Statistically optimal almost-invariant sets. Physica D **200**, 205 (2005)